JCTC Journal of Chemical Theory and Computation

Article

pubs.acs.org/JCTC

Meta-GGA Exchange-Correlation Functional with a Balanced Treatment of Nonlocality

Lucian A. Constantin,*[,†] E. Fabiano,[‡] and F. Della Sala[†,‡]

[†]Center for Biomolecular Nanotechnologies @UNILE, Istituto Italiano di Tecnologia (IIT), Via Barsanti, 73010 Arnesano (LE), Italy

[‡]National Nanotechnology Laboratory (NNL), Istituto Nanoscienze-CNR, Via per Arnesano 16, 73100 Lecce, Italy

Supporting Information

ABSTRACT: We construct a meta-generalized-gradient approximation which properly balances the nonlocality contributions to the exchange and correlation at the semilocal level. This nonempirical functional shows good accuracy for a broad palette of properties (thermochemistry, structural properties) and systems (molecules, metal clusters, surfaces, and bulk solids). The accuracy for several well-known problems in electronic structure calculations, such as the bending potential of the silver trimer and the dimensional crossover of anionic gold clusters, is also demonstrated. The inclusion of empirical dispersion corrections is finally discussed and analyzed.

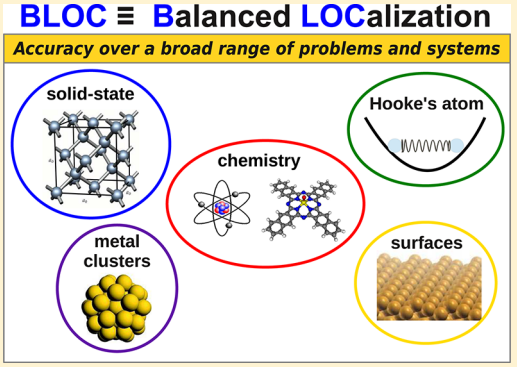

INTRODUCTION

The exchange-correlation (XC) energy functional is the key quantity in Kohn−Sham density functional theory (DFT)[1] and it is subject to intense research.[2] The simplest functionals of practical utility are those based on the generalized gradient approximation (GGA) which are constructed using the electron density and its gradient. At present, there exist GGA functionals that are rather accurate for molecules,[3−7] solids,[8,9] interfaces,[10] and even low-dimensional systems.[11] However, in general no GGA functional can be simultaneously accurate for many of these problems,[12] due to the extreme simplicity of the GGA level. Meta-generalized-gradient approximations (meta-GGAs)[13−20] are the most sophisticated semilocal functionals, incorporating important exact conditions and having an improved overall accuracy with respect to the GGA functionals, with almost the same attractive computational cost. These functionals use as an additional ingredient to the GGA ones, the kinetic energy density $\tau(\mathbf{r})$, which enters in the expansion of the angle-averaged exact exchange hole,[21] thus being a natural and important tool in the construction of XC approximations.

In this field, recently we proposed a meta-GGA dynamical correlation functional (named TPSSloc),[22] which takes advantage of an increased localization scheme for the correlation energy density. The TPSSloc correlation has the same form as TPSS[13] but uses as an ingredient a localized version of the PBE correlation functional[3] (named PBEloc), having the physically motivated correlation parameter (atomic units are used throughout)

$$\beta(r_s, t) = \beta_0 + at^2(1 - e^{-r_s^2}) \quad (1)$$

with $\beta_0 = 0.0375$ obtained from the linear response of the local density approximation (LDA),[1] $a = 0.08$ obtained by jellium surface analysis (so that PBEloc/TPSSloc can correctly describe quantum effects at the edges of electronic systems[23]), $t = |\nabla n|/2k_s\phi n$,[24] $k_s = (4k_F/\pi)^{1/2}$ being the Thomas−Fermi screening wave vector ($k_F = (3\pi^2 n)^{1/3}$), $r_s = [3/(4\pi n)]^{1/3}$ being the local Seitz radius, and $\phi = ((1 + \zeta)^{2/3} + (1 - \zeta)^{2/3})/2$ being a spin-scaling factor.[25,26] The TPSSloc correlation functional is very accurate for the description of correlation effects in the Hooke's atom at all confinement regimes, has an accurate and realistic short-range correlation hole, and for this reason is more compatible with exact exchange than the TPPS[13] or revTPSS[14] correlation functionals. In a previous work,[22] we used the TPSSloc correlation functional in combination with the revTPSS exchange, obtaining good results for systems where the exact XC hole is localized (atomization energies, kinetics, and bond lengths of small molecules). This approach is however of limited general applicability because, since the TPSSloc correlation hole density is strongly localized around the electron, for broad applicability it needs to be paired with an exchange functional which performs (at least) as well as revTPPS exchange for problems displaying a reduced nonlocality but also properly describes the missing nonlocality effects. Such an exchange functional should account for most of the tail XC hole effects[27] and the static correlation present in electronic systems near the equilibrium, which can be well captured by semilocal functionals. We recall that semilocal exchange functionals describe nonlocality effects through a proper shape of the enhancement factor, especially at medium

Received: February 27, 2013
Published: April 9, 2013

and large values of the reduced gradient for exchange $s = |\nabla n|/2k_F n$, also containing static correlation that scales as exchange under the uniform scaling of the density, which is essential for the description of electronic systems with more delocalized density.[28]

In this article, we consider this problem, and we introduce a nonempirical meta-GGA exchange functional with balanced nonlocality contributions that is fully compatible with the TPSSloc correlation functional. The resulting XC functional with balanced localization is named BLOC. Because of a better separation and proper balancing of exchange, dynamical correlation, and long-range XC effects, can achieve a good accuracy over a broad range of problems, correcting most of the XC TPSSloc limitations. In addition, to account for dispersion-related problems, which cannot be described by our localized correlation nor through the exchange nonlocality, we include a semiempirical dispersion correction[29] to the functional, obtaining the BLOC-D3 functional.

THEORY

As a starting point of our construction, we consider the TPSS and revTPSS exchange functionals, having the form

$$E_x[n] = \int \mathrm{d}\mathbf{r}\, n\varepsilon_x^{\mathrm{LDA}} F_x \tag{2}$$

with $\varepsilon_x^{\mathrm{LDA}}$ being the LDA exchange energy per particle[1] and F_x the exchange enhancement factor[13]

$$F_x = 1 + \kappa - \kappa/(1 + x/\kappa) \tag{3}$$

The parameter $\kappa = 0.804$ is fixed from the Lieb−Oxford bound,[30] while

$$x = \left\{\left[\frac{10}{81} + c\frac{z^f}{(1+z^2)^2}\right]s^2 + \frac{146}{2025}\tilde{q}_b^2 - \frac{73}{405}\tilde{q}_b\sqrt{\frac{1}{2}\left(\frac{3}{5}z\right)^2 + \frac{1}{2}s^4} + \frac{1}{\kappa}\left(\frac{10}{81}\right)^2 s^4 + 2\sqrt{e}\frac{10}{81}\left(\frac{3}{5}z\right)^2 + e\mu s^6\right\}/(1 + \sqrt{e}s^2)^2 \tag{4}$$

is constructed to recover the fourth-order gradient expansion (GE4) of the exchange energy,[13] for a slowly varying density. Here, $z = \tau^W/\tau$ $(0 \le z \le 1)$ is the meta-GGA ingredient[13] that distinguishes the iso-orbital regions (when $z \to 1$) and the slowly varying regime (when $z \to 0$), with $\tau^W = |\nabla n|^2/(8n)$ being the von Weizsäcker kinetic energy density and τ the Kohn−Sham positive kinetic energy density. s is the reduced gradient for exchange, and $\tilde{q}_b = (9/20)(\alpha - 1)/(1 + 0.4\alpha(\alpha - 1))^{1/2} + 2s^2/3$ mimics the reduced Laplacian of the density $q = \nabla n^2/(4(3\pi^2)^{2/3}n^{5/3})$, with $\alpha = (\tau - \tau^W)/\tau^{\mathrm{unif}} = (5/3)s^2(1/z - 1)$. The parameters c and e were fixed from the constraint that the exchange potential should be finite near the nucleus (where $z = 1$ and $s \approx 0.4$) and by fitting the exchange energy of the hydrogen atom (where $z = 1$).[13,14] The parameter μ dictates the behavior of the functional at large s ($s \gtrsim 2$), i.e., in valence and tail regions. In TPSS, $\mu = 0.21951$, which represents the nonempirical PBE value, whereas in revTPSS, $\mu = 0.14$ was set from semiempirical considerations. Finally, the parameter f controls the slowly varying behavior of the meta-GGA: when f is small (e.g., $f = 2$ in TPSS), the functional recovers GE4 only when s is very small ($s \lesssim 0.1$); when f is larger (e.g., $f = 3$ in revTPSS), the functional recovers GE4 over a broader range of s values ($s \lesssim 0.3$) and thus gains improved accuracy for bulk solids.[14]

Due to many successful applications of TPSS and revTPSS, the ansatz of eq 4 has been proved to be very robust in its general form. Thus, it provides an ideal starting point for building our new meta-GGA functional through selected modifications and improvements. We recall that this is a common practice in functional development, so for example the TPSS meta-GGA was developed on the skeleton of the PKZB meta-GGA precursor,[18] whereas revTPSS is just a judicious modification to TPSS, which brings new physical ideas. We also acknowledge the very recent work[16] into the direction of simplifying eq 4 and solving the order of limits problem. However, this new development, despite its conceptual importance, does not appear, at present, to improve considerably for practical molecular applications. Therefore, it will not be considered in the present work.

We build our exchange functional using eqs 2, 3, and 4, and we fix the μ parameter to its nonempirical PBE and TPSS value of 0.21951. In this way, the good TPSS description at large s values, i.e. in the outer-valence and tail regions, is recovered. Moreover, imposing the known meta-GGA constraints[13] for the hydrogen atom, we also have $c = 1.59096$ and $e = 1.537$. Note that these parameters are fixed only by constraints implying $z = 1$, and thus they cannot optimize the functional for the slowly and moderately varying density regimes, i.e. for short- and partially long-range effects. This behavior is instead controlled by the value of f, which determines how fast, for $s \to 0$, GE4 is recovered,[14] and also the behavior of the functional in the valence regions where $0.6 \lesssim z < 1$ and s is moderately large. Thus, a proper choice of f is crucial for the compatibility between exchange and correlation parts, being able to modulate both short- and long-range effects.

In our construction, we adopt therefore a flexible choice for f and generalize it to be a linear function of z (i.e., $f(z) = az + b$). Note that z is always finite $(0 \le z \le 1)$, and it is a good indicator for iso-orbital regions (where $z \approx 1$) as well as for the slowly varying regime (where $z \approx 5s^2/3 \ll 1$). We specify the following properties:

(i) $f(z) \ge 3$ for $z \le 0.3$. This condition ensures the recovery of GE4 over a wide range of s values, and thus the functional can be accurate for bulk solids,[14] granting a good description of short-range effects. Note that $z \le 0.3$ in most of the bulk solids, where the density is slowly varying.

(ii) $f(z) \le 2$ for $z \ge 0.6$. This constraint dictates the behavior of the functional in rapidly varying regions, giving $F_x \ge F_x^{\mathrm{TPSS}}$ in valence and tail regions.

(iii) As for the TPSSloc correlation, we take the jellium surfaces as a reference system. Thus, we require the exchange functional to complement the TPSSloc correlation in such a way as to be in agreement with diffusion Monte Carlo (DMC) estimates[31,32] of jellium surface XC energies (i.e., $\sigma_{xc}^{\mathrm{BLOC}} \approx \sigma_{xc}^{\mathrm{DMC}}$). We consider the benchmark $\sigma_{xc}^{\mathrm{DMC}}$ given by eq 5 of ref 32.

Conditions i−iii are satisfied by the simple form

$$f(z) = 4 - 3.3z \tag{5}$$

which completes the construction of the desired exchange meta-GGA functional (BLOC exchange). We note that the form chosen for $f(z)$ is just a simple ansatz which can satisfy conditions i−iii, without any rigorous base in an "exact" theory. Nevertheless, it provides a simple but effective way to realize

the required balance between exchange and correlation and allows one to achieve good accuracy for the XC functional (see later on).

The resulting exchange enhancement factor is compared in Figure 1 (panels a and b) with the TPSS and revTPSS ones, for

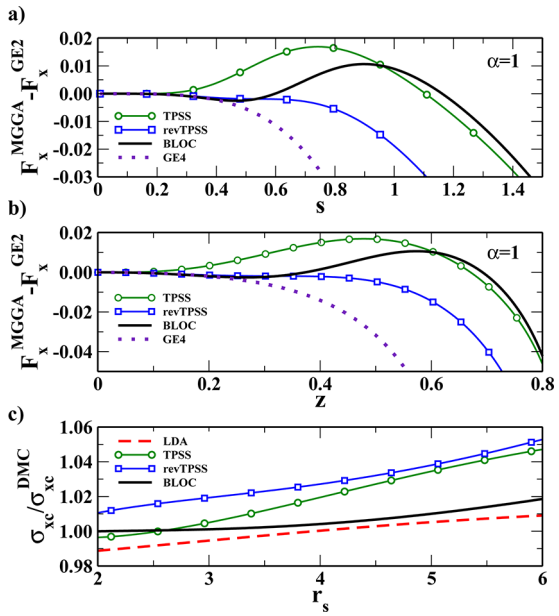

Figure 1. Comparison of the exchange enhancement factors of TPSS, revTPSS, GE4, and present exchange, in the case of $\alpha = 1$, with the second order gradient expansion $F_x^{GE2} = 1 + 10/81s^2$, versus the reduced gradient s (panel a) and z (panel b). Panel c shows the ratio of jellium surface XC energies $\sigma_{xc}^{approx}/\sigma_{xc}^{DMC}$ versus r_s, for several XC functional approximations.

$\alpha = 1$, i.e., in the case of slowly and moderately varying density regimes. The plot shows that the new exchange recovers GE4 until $s \leq 0.4$ or $z \leq 0.3$ (whereas revTPSS recovers GE4 until $s \leq 0.3$), being also very close to GE2 until $s \leq 0.6$ ($z \lesssim 0.4$), fulfilling condition i. For $s \geq 1$ and $z \geq 0.6$, the enhancement factor is slightly greater than TPSS, fulfilling condition ii.

We note that some of the features of the BLOC exchange may recall the recently proposed VT{8,4} meta-GGA exchange functional[17] that is well compatible with revTPSS correlation. Nevertheless, this exchange functional slightly de-enhances at $1 \leq s \leq 2$ and enhances at $s \geq 2.4$ over revTPSS (see Figure 2 of ref 17). Thus, we expect it to work similarly to the TPSSloc XC functional[22] when used together with the TPSSloc correlation.

To complete our analysis, panel c of Figure 1 reports the ratio of jellium surface XC energies σ_{xc} with respect to DMC results as a function of r_s. These data clearly show that the BLOC XC-functional is in best agreement with the DMC benchmark estimates (fulfilling condition iii). However, we stress that all the functionals presented in the figure (TPSS, revTPSS, BLOC, and LDA) are very accurate for jellium XC surface energies.

Beyond conditions i−iii, the proposed construction of the BLOC exchange carries important physical content and goes beyond the simple need to complement the TPSSloc correlation. In fact, it shares most of the good features of TPSS and revTPSS exchange. Moreover, by construction, for any one- and two-electron systems (where $z = 1$), the BLOC exchange functional exactly recovers the TPSS one, which is known to be a very accurate meta-GGA model for exchange in such systems (being closer to the conventional exact exchange energy density than the revTPSS one[14]). Thus, BLOC exchange (as all the other nonempirical meta-GGAs) has as a target model system also the hydrogen atom (note that TPSSloc correlation correctly vanishes for any one-electron system).

Additionally, Figure 2 shows that the BLOC XC functional preserves, and even improves, the performance of the TPSSloc

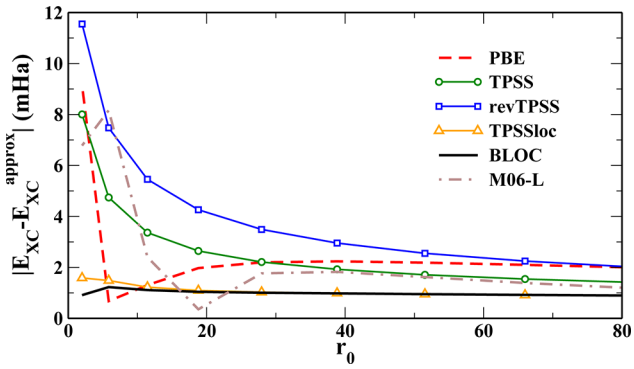

Figure 2. Absolute error for the exchange-correlation energy of the Hooke's atom at different values of the classical electron distances $r_0 = (\omega^2/2)^{-1/3}$, with ω being the frequency of the isotropic harmonic potential. The electrons are tightly bound at small r_0 and are strongly correlated at large r_0.

functional for the Hooke's atom, especially in the tightly bounded region, outperforming all the reported meta-GGAs (TPSS, revTPSS, and M06-L[19]). We recall that the Hooke's atom[22,33−36] represents two interacting electrons in an isotropic harmonic potential. Thus, a good description of both two-electron exchange and correlation is required. This model system provides deep physical insight into strongly correlated and tightly bounded regimes, being an important and hard test for density functionals.

Finally, in Figure 3 we show a comparison of the TPSS, revTPSS, and BLOC exchange (upper panel) and XC (lower panel) energy densities, at a jellium surface of bulk parameter r_s

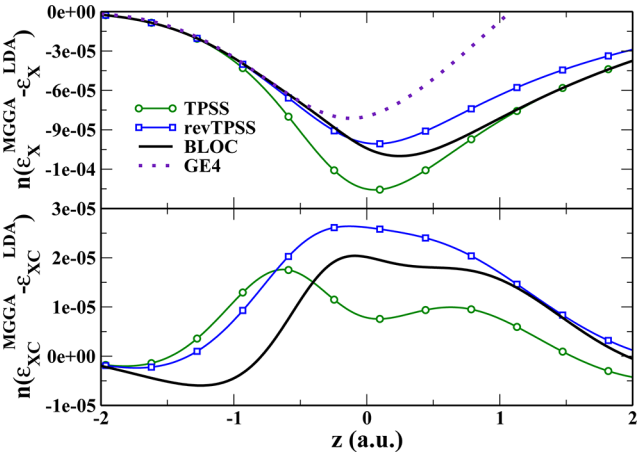

Figure 3. Upper panel: GE4, TPSS, revTPSS, and BLOC exchange energy densities with respect to LDA ($n(\varepsilon_x - \varepsilon_x^{LDA})$), versus the distance z, for a semi-infinite jellium surface of bulk parameter $r_s = 2$. The surface is at $z = 0$, the bulk is at $z \leq 0$, and the vacuum is at $z \geq 0$. Lower panel: TPSS, revTPSS, and BLOC exchange-correlation energy densities with respect to LDA ($n(\varepsilon_{xc} - \varepsilon_{xc}^{LDA})$), for the same system.

Table 1. Mean Absolute Errors for Various Tests As Resulting from TPSS, revTPSS, TPSSloc, BLOC, and BLOC-D3 meta-GGAs Calculations[a]

test set	TPSS	revTPSS	TPSSloc	BLOC	BLOC-D3	M06-L
atomization energies and proton affinities (kcal/mol)						
organic molecules (AE6)	5.4	6.6	3.9	3.6	3.6	3.4
organic molecules (W4-NMR)	4.7	5.2	5.5	4.6	4.4	5.4
static correlation (W4-MR)	8.8	9.4	14.0	8.9	9.1	5.9
proton affinities (PA12)	4.7	4.8	3.8	3.7	3.8	4.5
RMAE	**1.00**	**1.10**	**1.07**	**0.86**	**0.86**	**0.85**
reaction energies and kinetics (kcal/mol)						
organic molecules (OMRE)	8.0	10.2	7.9	7.1	6.0	5.3
kinetics (K9)	7.0	7.2	6.5	6.3	6.4	4.2
barrier height (BH6)	8.3	7.4	8.6	8.9	8.9	4.3
RMAE	**1.00**	**1.07**	**0.98**	**0.95**	**0.91**	**0.59**
other (kcal/mol)						
ionization pot. (IP13)	3.1	2.9	3.0	3.3	3.3	3.1
isomerization (ISOL6)	3.6	4.0	2.7	3.5	3.0	2.8
difficult cases (DC9/12)	18.2	21.7	29.6	20.1	19.4	22.3
atomic energies (AE17)	22.6	41.8	42.4	26.8	26.8	3.9
RMAE	**1.00**	**1.27**	**1.31**	**1.08**	**1.04**	**0.79**
noncovalent interactions (kcal/mol)						
hydrogen bonding (HB6)	0.6	0.6	0.6	0.6	0.8	0.6
dipole bonding (DI6)	0.6	0.5	0.5	0.5	0.8	0.4
$\pi-\pi$ stacking (PPS5)	2.8	2.5	2.7	2.8	0.1	0.8
various noncovalent (S22)	3.2	2.8	2.6	3.3	0.5	0.6
RMAE	**1.00**	**0.90**	**0.90**	**0.97**	**0.71**	**0.53**
structural properties (mÅ and cm^{-1})						
bond lengths (MGBL19)	6.9	7.4	6.8	5.9	5.7	3.0
vibrations (F38)	44.1	43.7	41.9	39.0	40.0	41.5
RMAE	**1.00**	**1.03**	**0.97**	**0.87**	**0.87**	**0.69**
transition metals (mÅ, kcal/mol (TM10AE), and kcal/mol/atom (AUnAE))						
transition-metal energies (TM10AE)	10.8	11.1	10.3	11.1	11.0	7.9
gold cluster energies (AUnAE)	0.6	1.6	4.4	0.3	0.4	1.4
transition-metal geom. (TMBL)	12.7	11.6	17.7	11.2	11.3	10.9
gold cluster geom. (AuBL6)	30.8	21.9	35.3	23.3	19.6	33.9
RMAE	**1.00**	**1.33**	**2.71**	**0.79**	**0.80**	**1.26**
global assessment for chemical properties						
average RMAE	**1.00**	**1.12**	**1.32**	**0.92**	**0.87**	**0.79**
bulk solids (Å, GPa, and eV/atom)						
lattice constants (LC12)	0.056	0.043	0.049	0.048		0.057
bulk moduli (BM12)	7.8	9.4	15.7	7.8		10.5
cohesive energies (COH12)	0.131	0.162	0.385	0.117		0.358
RMAE	**1.00**	**1.07**	**1.94**	**0.92**		**1.70**

[a]M06-L results are also reported for reference. The BLOC results are underlined whenever they equate to or are better than both TPSS and revTPSS. For each group of tests, the mean absolute errors relative to TPSS (RMAEs) are reported in the last line. Full results are reported in the Supporting Information.[43].

= 2. The BLOC exchange energy density is smooth and performs in accord with conditions i–iii: inside the bulk, where the density is slowly varying, it recovers GE4 better than revTPSS, whereas in the vacuum, where the density starts to vary rapidly, it is close to TPSS. Note that GE4 fails badly in the tail of density. On the other hand, the BLOC XC energy density is *qualitatively* different from both TPSS and revTPSS, because of the stronger localization of the correlation and of the short-range exchange.

COMPUTATIONAL DETAILS

To assess the performance of the BLOC functional for real problems, we implemented it into development versions of the TURBOMOLE[37] and FHI-AIMS[38,39] program packages. The two programs were used for all molecular and solid-state calculations, using def2-TZVPP[40,41] and third tier[38] basis sets, respectively. All molecular and metal-cluster calculations are self-consistent, whereas the bulk solids calculations were performed using PBEsol orbitals and densities. A similar non-self-consistent approach (using LDA orbitals) was used in refs 14 and 42. Moreover, we have found that the solid-state results are insensitive to the choice of the orbitals (as also shown in ref 42). The moderately large basis sets were chosen to provide an optimal compromise between accuracy and computational cost, so that our results can be directly transferable to practical applications. We note also that the use of the same basis set for all the functionals in Table 1 should provide a fair assessment of relative performances. An analysis of the basis set accuracy for the AE6 test is reported in the Supporting Information.[43]

We considered a set of representative and widely used tests (including overall more than 300 systems), which were divided into seven groups:

- **Atomization energies and proton affinities of organic molecules**, which includes the W4[44−46] and PA12[45,46] test sets. Moreover, the AE6 test[47] for atomization energies was also chosen, because this small representative test is often used to benchmark quantum chemistry methods and provides therefore a direct comparison with many other works. Finally, the W4-MR test,[44] of molecules with nonsingle-reference character, was considered for completeness.
- **Reaction energies and kinetics**, including representative tests for organic reaction energies (OMRE[48]), barrier heights (BH6[47]), and both (K9[49]).
- **Other** tests, which are relevant for assessing density functionals: ionization potentials (IP13[50]), isomerization energies (ISOL6[51]), difficult cases for DFT (DC9/12[52]), and absolute atomic energies (AE17[19]).
- **Noncovalent interactions**, comprising tests for hydrogen bonds (HB6[53]), dipole−dipole interactions (DI6[53]), $\pi-\pi$ stacking (PPS5[53]), and the S22 test,[45,46] which includes a broad selection of noncovalent interactions.
- **Structural properties** of organic molecules. This group includes a test of optimized bond lengths (MGBL19[54]) and one test of harmonic vibrational frequencies (F38[55]).
- **Transition metals**. In this group, we collected a set of tests involving transition metal complexes (TM10AE[25] for atomization energies and TMBL[56] for bond lengths) and gold clusters (AunAE[25,57] for atomization energies and AuBL6[57] for bond lengths).
- **Bulk solids**. This group includes the tests of the equilibrium lattice constants (LC12), bulk moduli (BM12), and cohesive energies (COH12) of 12 bulk solids: Li, Na, and Al (simple metals); Cu, Ag, and Pd (transition metals); Si, Ge, and GaAs (semiconductors); and NaCl, NaF, and MgO (ionic solids). The reference data were taken from 42.

To assess the performance of different functionals for each group of tests we consider, besides the individual mean absolute error (MAE) for each test, an overall MAE relative to TPSS (RMAE), defined as[58]

$$\mathrm{RMAE} = \frac{1}{M}\sum_{i}^{M}\frac{\mathrm{MAE}_i}{\mathrm{MAE}_i^{\mathrm{TPSS}}} \tag{6}$$

where the sum runs over all tests (M) within a group and $\mathrm{MAE}_i^{\mathrm{TPSS}}$ is the MAE of TPSS for the ith test. The RMAE provides an indication of whether any method is better (RMAE < 1) or worse (RMAE > 1) than TPSS for a given problem. Thus, it allows a fair global assessment of all the results.

Finally, in addition to the tests listed above, we considered two special cases which are known to be difficult for semilocal density functionals, namely the description of the bending potential of the silver trimer[59,60] and the dimensional crossover of gold anionic clusters.[61−64]

RESULTS

The results of all tests are summarized in Table 1 where we report the MAEs and RMAEs for different tests and groups as resulting from different functionals. The TPSS and revTPSS results are considered for direct comparison with parent nonempirical functionals. The M06-L results are also reported, to have a reference of a widely used and highly parametrized meta-GGA functional.

Inspection of Table 1 shows that BLOC performs better than both revTPSS and TPSS in more than 60% of the tests. On the other hand, it compares also relatively well with the "benchmark" M06-L results, yielding lower MAEs in 30% of the cases and giving significantly worse results only in two cases (atomic energies and barrier heights). Even though this performance may not appear to be outstanding at first sight, we remind the reader of the difficulty of outperforming highly parametrized meta-GGA functionals without resorting to higher nonempirical rungs of the DFT Jacob's ladder.[65] At the same time, the comparison of BLOC, TPSS, and revTPSS results shows how difficult it is to reach a good accuracy at the meta-GGA level, for a broad range of properties, without introducing a high level of empiricism. In this sense, the good performance of BLOC is quite satisfactory, and its rather systematic improvement over TPSS and revTPSS indicates that the functional captures well the essential physics of a wide selection of electronic systems at the simple semilocal level. Thus, the balanced description of different regimes and the physical concepts included in exchange and correlation parts of the BLOC functional are relevant.

In particular, we underline here the good performance of the BLOC functional for the structural properties of molecules, atomization energies/proton affinities, and all the properties of transition metal systems. On the other hand, in only three cases (BH6, IP13, S22) BLOC is worse than both revTPSS and TPSS (still being very close to the TPSS). Moreover, at least two of these tests (BH6, S22) can hardly be accurate for nonempirical semilocal functionals. We also remark that HF +TPSSloc is extremely good for BH6 (see Table 1 of ref 22), and thus we expect that a hybrid of the BLOC functional can be rather accurate for barrier heights.

Overall, BLOC has the second best RMAE (0.92) for chemical properties and the best RMAE for bulk solids (0.92). Note that the M06-L functional is the best for molecular properties, but it is modest for solids. The more recent M11-L functional[20] improves lattice constants, but not solid-state cohesive energies.[66] In fact, even revTPSS improves over TPSS for lattice constants but worsens both bulk moduli and cohesive energies (see Table 1 and also ref 67). On the other hand, BLOC gives a very good balance for all solid-state properties.

We remark also that notably these results can be in general obtained with a small error compensation for situations where the XC hole is reasonably localized (e.g., for the AE6 test), because of the higher compatibility of the TPSSloc correlation with exact exchange.[22] In these cases in fact TPSSloc and BLOC correctly yield very close results. On the other hand, for systems characterized by delocalized electrons and/or static correlation, our balanced exchange functional proves to be capable of compensating well for the missing long-tail behavior of the TPSSloc correlation, so that good results can be finally obtained using the BLOC XC functional (see e.g. W4-MR, DC9/12, AunAE, and COH12).

The results of Table 1 show (second last column) that a small further improvement can be achieved by complementing the BLOC functional with semiempirical dispersion corrections. In fact, dispersion cannot be described by the localized TPSSloc correlation nor can it be included in the exchange part. We implemented this correction through the DFT-D3 semi-empirical model,[29] fixing the two free parameters of the model by fitting to the MAE of the S22 test. The resulting parameters are $s_{r,6} = 1.104$ and $s_8 = 0.888$, slightly smaller than the TPSS values. We see that the BLOC-D3 functional of

course strongly improves the performance for dispersion-dominated tests (e.g., S22, PPS5) but, at the same time, also preserves the accuracy for all other tests, even slightly improving the MAE in some cases (e.g., structural properties, W4, OMRE). Thus, the semiempirical DFT-D3 correction appears to integrate well with our construction, and as a result the BLOC-D3 functional yields a very good performance for chemistry-related tests (RMAE = 0.87).

Silver Trimer. As an additional test for our assessment of the BLOC functional, we consider a particularly difficult case for DFT: the description of the potential energy related to the bending of the Ag_3 cluster.[59,60] For this case, in fact high-level methods indicate the existence of a single minimum at a bond angle of $\theta \approx 70°$, whereas all PBE-based functionals yield two almost degenerate minima at $\theta \approx 70°$ and at $\theta \approx 140°$,[59] and all LYP-based functionals yield only the wrong 140° minimum. The results reported in Figure 4 show indeed that the popular

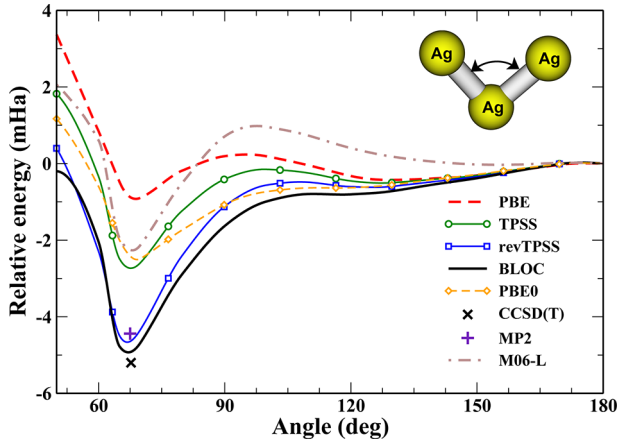

Figure 4. Relative energy (in mHa) with respect to the linear structure of Ag_3 ($\Delta E = E(\theta) - E(180°)$) as a function of the Ag−Ag−Ag bond angle θ (in degrees) for several functionals. CCSD(T) and MP2 values are taken from ref 60.

PBE and even the meta-GGA TPSS or the hybrid PBE0 functionals yield a poor quantitative description of the problem, where the relative energy of the global minimum is underestimated, and only by the inclusion of exact exchange can the second minimum at $\theta \approx 140°$ be turned into a shoulder. On the other hand, revTPPS yields a good relative energy for the minimum at $\theta \approx 70°$ but still displays a small second minimum at $\theta \approx 140°$, due to a hill at ∼100°. The BLOC functional instead gives a very good description of the bending potential of the Ag_3 cluster in good agreement with CCSD(T) calculations,[60] transforming the hill at ∼100° into a shoulder. We note finally that, for this problem, highly empirical meta-GGAs (as M06-L) are also rather inaccurate (as shown in Figure 4).

The Dimensional Transition of Anionic Gold Clusters Problem. Finally, we consider the problem of the two-dimensional to three-dimensional (2D→3D) transition in gold cluster anions, which attracted great interest over the past several years.[61−64,68,69] A joint electron diffraction and DFT study[61] showed in fact that the 2D→3D transition occurs for Au_n^- clusters at $n = 12$, where a 2D and a 3D structure are almost isoenergetic, while planar (2D) and 3D structures characterize the experimental spectrum for $n = 11$ and $n = 13$, respectively. However, most DFT functionals are unable to reproduce this outcome.[61,68,69]

In Table 2, we show the relative energies of several 2D and 3D gold clusters as obtained from several meta-GGA

Table 2. Relative Energies (meV) with Respect to Conformer I of 2D and 3D Gold Cluster Anions with 11−13 Atoms[a]

system	dim[b]	TPSS	revTPSS	TPSSloc	BLOC	M06-L[c]
Au_{11}^--I	2D	0	0	0	0	0
Au_{11}^--II	3D	190	159	121	190	60
Au_{11}^--III	3D	270	337	419	310	250
Au_{12}^--I	3D	0	0	0	0	0
Au_{12}^--II	2D	−170	79	343	37	400
Au_{13}^--I	3D	0	0	0	0	0
Au_{13}^--II	3D	10	39	65	29	110
Au_{13}^--III	2D	230	467	766	426	930

[a]The structures of the clusters and the nomenclature can be found in ref 61. All energies include the correction terms reported in Table IV of ref 61, in order to account for spin-orbit, all-electron, zero-point vibrational energy, and thermal effects. [b]Dimensionality. [c]Data from ref 68.

functionals. The TPSS functional erroneously predicts the 2D structure to be favorable at $n = 12$ (as most GGA functionals, including PBE[3,57]). The other meta-GGAs (revTPSS, TPSSloc, BLOC, and M06-L), on the other hand, correctly solve the dimensional crossover of anionic gold clusters. However, only the revTPSS and BLOC meta-GGAs predict almost isoenergetic structures for Au_{12}^--I and Au_{12}^--II, in better agreement with experimental results,[61] and with the M06 hybrid functional.[68]

CONCLUSIONS

In conclusion, we constructed an accurate, nonempirical, and physically motivated meta-GGA XC functional. Its dynamical correlation part is strongly localized, showing a realistic short-range correlation and being more compatible with exact exchange than other popular correlation functionals.[22] The exchange part was constructed to balance nonlocality effects at the semilocal exchange level, so as to have a good description of different density regimes in different systems. Additional inclusion of dispersion effects can be efficiently obtained via semiempirical corrections.

Nowadays, highly empirical functionals are optimized against a large set of data and chemical properties,[19] and thus they become very attractive for many electronic structure calculations. However, due to their empirical nature, they may show unexpected failures for specific or exotic problems. On the other hand, the nonempirical functionals, constructed from exact quantum mechanics conditions and from model systems, show a reasonable accuracy for most applications, due to the physics which they incorporate. The BLOC meta-GGA improves over, or is in line with, state-of-the-art TPSS and revTPSS for many energetic and structural properties of organic molecules, transition metal complexes and clusters, jellium surfaces, Hooke's atom, and bulk solids and can correctly solve difficult problems such as the bending potential of the silver trimer and the dimensional crossover in gold anionic clusters and thus can become a nonempirical workhorse tool in quantum chemistry and condensed matter.

■ ASSOCIATED CONTENT

Supporting Information

Basis set dependence of the AE6 test and full results of Table 1. This material is available free of charge via the Internet at http://pubs.acs.org/.

■ AUTHOR INFORMATION

Corresponding Author

*E-mail: lucian.constantin@iit.it.

Notes

The authors declare no competing financial interest.

■ ACKNOWLEDGMENTS

This work was partially funded by the European Research Council (ERC) Starting Grant FP7 Project DEDOM, Grant No. 207441. We thank TURBOMOLE GmbH for providing the TURBOMOLE program package and M. Margarito for technical support.

■ REFERENCES

(1) Kohn, W.; Sham, L. J. Self-Consistent Equations Including Exchange and Correlation Effects. *Phys. Rev.* **1965**, *140*, A1133−A1138.

(2) Scuseria, G. E.; Staroverov, V. N. Progress in the development of exchange-correlation functionals. In *Theory and Applications of Computational Chemistry:The First Forty Years*; Dykstra, C., Frenking, G., Kim, K., Scuseria, G., Eds.; Elsevier Science: Berlin, 2005; pp 669−724.

(3) Perdew, J. P.; Burke, K.; Ernzerhof, M. Generalized Gradient Approximation Made Simple. *Phys. Rev. Lett.* **1996**, *77*, 3865−3871.

(4) Constantin, L. A.; Fabiano, E.; Laricchia, S.; Della Sala, F. Semiclassical neutral atom as a reference system in density functional theory. *Phys. Rev. Lett.* **2011**, *106*, 186406−186410.

(5) Tognetti, V.; Cortona, P.; Adamo, C. A new parameter-free correlation functional based on an average atomic reduced density gradient analysis. *J. Chem. Phys.* **2008**, *128*, 034101−034109.

(6) Vela, A.; Pacheco-Kato, J. C.; Gázquez, J. L.; del Campo, J. M.; Trickey, S. B. Improved constraint satisfaction in a simple generalized gradient approximation exchange functional. *J. Chem. Phys.* **2012**, *136*, 144115−144123.

(7) del Campo, J. M.; Gázquez, J. L.; Trickey, S. B.; Vela, A. Non-empirical improvement of PBE and its hybrid PBE0 for general description of molecular properties. *J. Chem. Phys.* **2012**, *136*, 104108−104116.

(8) Perdew, J. P.; Ruzsinszky, A.; Csonka, G. I.; Vydrov, O. A.; Scuseria, G. E.; Constantin, L. A.; Zhou, X.; Burke, K. Restoring the Density-Gradient Expansion for Exchange in Solids and Surfaces. *Phys. Rev. Lett.* **2008**, *100*, 136406−136410.

(9) Armiento, R.; Mattsson, A. E. Functional designed to include surface effects in self-consistent density functional theory. *Phys. Rev. B* **2005**, *72*, 085108−085113.

(10) Fabiano, E.; Constantin, L. A.; Della Sala, F. Generalized gradient approximation bridging the rapidly and slowly varying density regimes: A PBE-like functional for hybrid interfaces. *Phys. Rev. B* **2010**, *82*, 113104−113108.

(11) Chiodo, L.; Constantin, L. A.; Fabiano, E.; Della Sala, F. Nonuniform scaling applied to surface energies of transition metals. *Phys. Rev. Lett.* **2012**, *108*, 126402−126406.

(12) Elliott, P.; Lee, D.; Cangi, A.; Burke, K. Semiclassical Origins of Density Functionals. *Phys. Rev. Lett.* **2008**, *100*, 256406−256410.

(13) Tao, J.; Perdew, J. P.; Staroverov, V. N.; Scuseria, G. E. Climbing the Density Functional Ladder: Nonempirical Meta-Generalized Gradient Approximation Designed for Molecules and Solids. *Phys. Rev. Lett.* **2003**, *91*, 146401−146405.

(14) Perdew, J. P.; Ruzsinszky, A.; Csonka, G. I.; Constantin, L. A.; Sun, J. Workhorse semilocal density functional for condensed matter physics and quantum chemistry. *Phys. Rev. Lett.* **2009**, *103*, 026403−026407; (Erratum) *Phys. Rev. Lett.* **2011**, *106*, 179902.

(15) Ruzsinszky, A.; Sun, J.; Xiao, B.; Csonka, G. I. A meta-GGA Made Free of the Order of Limits Anomaly. *J. Chem. Theory Comput.* **2012**, *8*, 2078−2087.

(16) Sun, J.; Xiao, B.; Ruzsinszky, A. Communication: Effect of the orbital-overlap dependence in the meta generalized gradient approximation. *J. Chem. Phys.* **2012**, *137*, 051101.

(17) del Campo, J. M.; Gázquez, J. L.; Trickey, S. B.; Vela, A. A new meta-GGA exchange functional based on an improved constraint-based GGA. *Chem. Phys. Lett.* **2012**, *543*, 179−183.

(18) Perdew, J. P.; Kurth, S.; Zupan, A.; Blaha, P. Accurate Density Functional with Correct Formal Properties: A Step Beyond the Generalized Gradient Approximation. *Phys. Rev. Lett.* **1999**, *82*, 2544−2548.

(19) Zhao, Y.; Truhlar, D. G. The M06 suite of density functionals for main group thermochemistry, thermochemical kinetics, noncovalent interactions, excited states, and transition elements: two new functionals and systematic testing of four M06-class functionals and 12 other functionals. *Theor. Chem. Acc.* **2008**, *120*, 215−241.

(20) Peverati, R.; Truhlar, D. G. M11-L: A Local Density Functional That Provides Improved Accuracy for Electronic Structure Calculations in Chemistry and Physics. *J. Phys. Chem. Lett.* **2012**, *3*, 117−124.

(21) Becke, A. D. Hartree-Fock exchange energy of an inhomogeneous electron gas. *Int. J. Quantum Chem.* **1983**, *23*, 1915−1922.

(22) Constantin, L. A.; Fabiano, E.; Della Sala, F. Semilocal dynamical correlation with increased localization. *Phys. Rev. B* **2012**, *86*, 035130−035135.

(23) Kohn, W.; Mattsson, A. E. Edge Electron Gas. *Phys. Rev. Lett.* **1998**, *81*, 3487−3491.

(24) Langreth, D. C.; Mehl, M. J. Easily Implementable Nonlocal Exchange-Correlation Energy Functional. *Phys. Rev. Lett.* **1981**, *47*, 446−450.

(25) Constantin, L. A.; Fabiano, E.; Della Sala, F. Improving atomization energies of molecules and solids with a spin-dependent gradient correction from one-electron density analysis. *Phys. Rev. B* **2011**, *84*, 233103−233108.

(26) Constantin, L. A.; Fabiano, E.; Della Sala, F. Spin-dependent gradient correction for more accurate atomization energies of molecules. *J. Chem. Phys.* **2012**, *137*, 194105−194113.

(27) Cohen, A. J.; Mori-Sánchez, P.; Yang, W. Challenges for Density Functional Theory. *Chem. Rev.* **2012**, *112*, 289−320.

(28) Cohen, A. J.; Mori-Sánchez, P.; Yang, W. Insights into Current Limitations of Density Functional Theory. *Science* **2008**, *321*, 792−794.

(29) Grimme, S.; Antony, J.; Ehrlich, S.; Krieg, H. A consistent and accurate ab initio parametrization of density functional dispersion correction (DFT-D) for the 94 elements H-Pu. *J. Chem. Phys.* **2010**, *132*, 154104−154123.

(30) Lieb, E. H.; Oxford, S. Improved lower bound on the indirect Coulomb energy. *Int. J. Quantum Chem.* **1981**, *19*, 427−439.

(31) Wood, B.; Hine, N. D. M.; Foulkes, W. M. C.; García-González, P. Quantum Monte Carlo calculations of the surface energy of an electron gas. *Phys. Rev. B* **2007**, *76*, 035403−035409.

(32) Constantin, L. A.; Pitarke, J. M.; Dobson, J. F.; García-Lekue, A.; Perdew, J. P. High-Level Correlated Approach to the Jellium Surface Energy, without Uniform-Gas Input. *Phys. Rev. Lett.* **2008**, *100*, 036401−036405.

(33) Taut, M. Two electrons in an external oscillator potential: Particular analytic solutions of a Coulomb correlation problem. *Phys. Rev. A* **1993**, *48*, 3561−3566.

(34) Filippi, C.; Umrigar, C. J.; Taut, M. Comparison of exact and approximate density functionals for an exactly soluble model. *J. Chem. Phys.* **1994**, *100*, 1290−1296.

(35) Filippi, C.; Gonze, X.; Umrigar, C. J. Generalized Gradient Approximations to Density Functional Theory: Comparison with Exact Results. In *Recent Developments and Applications of Modern*

Density Functional Theory; Seminario, J., Ed.; Elsevier Science: Berlin, 1996; Vol. *4*, pp 295−326.
(36) Constantin, L. A.; Chiodo, L.; Fabiano, E.; Bodrenko, I.; Della Sala, F. Correlation energy functional from jellium surface analysis. *Phys. Rev. B* **2011**, *84*, 045126−045136.
(37) *TURBOMOLE*, V6.3; TURBOMOLE GmbH: Karlsruhe, Germany, 2011. Available from http://www.turbomole.com (accessed April 2013).
(38) Blum, V.; Gehrke, R.; Hanke, F.; Havu, P.; Havu, V.; Ren, X.; Reuter, K.; Scheffler, M. Ab initio molecular simulations with numeric atom-centered orbitals. *Comput. Phys. Commun.* **2009**, *180*, 2175−2196.
(39) Havu, V.; Blum, V.; Havu, P.; Scheffler, M. Efficient O(N) integration for all-electron electronic structure using numerically tabulated basis functions. *J. Comput. Phys.* **2009**, *228*, 8367−8379.
(40) Weigend, F.; Furche, F.; Ahlrichs, R. Gaussian basis sets of quadruple zeta valence quality for atoms H-Kr. *J. Chem. Phys.* **2003**, *119*, 12753−12763.
(41) Weigend, F.; Ahlrichs, R. Balanced basis sets of split valence, triple zeta valence and quadruple zeta valence quality for H to Rn: Design and assessment of accuracy. *Phys. Chem. Chem. Phys.* **2005**, *7*, 3297−3305.
(42) Csonka, G.; Perdew, J. P.; Ruzsinszky, A.; Philipsen, P. H. T.; Lebègue, S.; Paier, J.; Vydrov, O. A.; Ángyán, J. G. Assessing the performance of recent density functionals for bulk solids. *Phys. Rev. B* **2009**, *79*, 155107−155121.
(43) See Supporting Information.
(44) Karton, A.; Tarnopolsky, A.; Lamére, J.-F.; Schatz, G. C.; Martin, J. M. L. Highly Accurate First-Principles Benchmark Data Sets for the Parametrization and Validation of Density Functional and Other Approximate Methods. Derivation of a Robust Generally Applicable, Double-Hybrid Functional for Thermochemistry and Thermochemical Kinetics. *J. Phys. Chem. A* **2008**, *112*, 12868−12886.
(45) Goerigk, L.; Grimme, S. A General Database for Main Group Thermochemistry, Kinetics, and Noncovalent Interactions − Assessment of Common and Reparameterized (meta-)GGA Density Functionals. *J. Chem. Theory Comput.* **2010**, *6*, 107−126.
(46) Goerigk, L.; Grimme, S. A thorough benchmark of density functional methods for general main group thermochemistry, kinetics, and noncovalent interactions. *Phys. Chem. Chem. Phys.* **2011**, *13*, 6670−6688.
(47) Lynch, B. J.; Truhlar, D. G. Small Representative Benchmarks for Thermochemical Calculations. *J. Phys. Chem. A* **2003**, *107*, 8996−8999.
(48) Fabiano, E.; Constantin, L. A.; Della Sala, F. Testing the broad applicability of the PBEint GGA functional and its one-parameter hybrid form. *Int. J. Quantum Chem.* **2012**, *13*, 6670−6688.
(49) Lynch, B. J.; Truhlar, D. G. Robust and Affordable Multicoefficient Methods for Thermochemistry and Thermochemical Kinetics: The MCCM/3 Suite and SAC/3. *J. Phys. Chem. A* **2003**, *107*, 3898−3906.
(50) Lynch, B. J.; Zhao, Y.; Truhlar, D. G. Effectiveness of Diffuse Basis Functions for Calculating Relative Energies by Density Functional Theory. *J. Phys. Chem. A* **2003**, *107*, 1384−1388.
(51) Luo, S.; Zhao, Y.; Truhlar, D. G. Validation of Electronic StructureMethods for Isomerization Reactions of Large Organic Molecules. *Phys. Chem. Chem. Phys.* **2011**, *13*, 13683−13689.
(52) Peverati, R.; Truhlar, D. G. Exchange-Correlation Functional with Good Accuracy for Both Structural and Energetic Properties while Depending Only on the Density and Its Gradient. *J. Chem. Theory Comput.* **2012**, *8*, 2310−2319.
(53) Zhao, Y.; Truhlar, D. G. Benchmark Databases for Nonbonded Interactions and Their Use To Test Density Functional Theory. *J. Chem. Theory Comput.* **2005**, *1*, 415−432.
(54) Zhao, Y.; Truhlar, D. G. A new local density functional for main-group thermochemistry, transition metal bonding, thermochemical kinetics, and noncovalent interactions. *J. Chem. Phys.* **2006**, *125*, 194101−194119.
(55) Biczysko, M.; Panek, P.; Scalmani, G.; Bloino, J.; Barone, V. Harmonic and Anharmonic Vibrational Frequency Calculations with the Double-Hybrid B2PLYP Method: Analytic Second Derivatives and Benchmark Studies. *J. Chem. Theory Comput.* **2010**, *6*, 2115−2125.
(56) Bühl, M.; Kabrede, H. Geometries of Transition-Metal Complexes from Density-Functional Theory. *J. Chem. Theory Comput.* **2006**, *2*, 1282−1290.
(57) Fabiano, E.; Constantin, L. A.; Della Sala, F. Exchange-correlation generalized gradient approximation for gold nanostructures. *J. Chem. Phys.* **2011**, *134*, 194112−194122.
(58) Fabiano, E.; Constantin, L. A.; Della Sala, F. Two-dimensional scan of the performance of generalized gradient approximations with Perdew-Burke-Ernzerhof-like enhancement factor. *J. Chem. Theory Comput.* **2011**, *7*, 3548−3559.
(59) Zhao, S.; Li, Z.-H.; Wang, W.-N.; Liu, Z.-P.; Fan, K.-N.; Xie, Y.; Schaefer, H. F., III. Is the uniform electron gas limit important for small Ag clusters? Assessment of different density functionals for Ag_n ($n \leq 4$). *J. Chem. Phys.* **2006**, *124*, 184102−184112.
(60) Huang, M.-J.; Watts, J. D. Theoretical study of triatomic silver (Ag_3) and its ions with coupled-cluster methods and correlation-consistent basis sets. *Phys. Chem. Chem. Phys.* **2012**, *14*, 6849−6855.
(61) Johansson, M. P.; Lechtken, A.; Schooss, D.; Kappes, M. M.; Furche, F. 2D-3D transition of gold cluster anions resolved. *Phys. Rev. A* **2008**, *77*, 053202−053209.
(62) Furche, F.; Ahlrichs, R.; Weis, P.; Jacob, C.; Gilb, S.; Bierweiler, T.; Kappes, M. M. The structures of small gold cluster anions as determined by a combination of ion mobility measurements and density functional calculations. *J. Chem. Phys.* **2002**, *117*, 6982−6990.
(63) Häkkinen, H.; Yoon, B.; Landman, U.; Li, X.; Zhai, H. -J.; Wang, L.-S. On the Electronic and Atomic Structures of Small Au_N^- (N = 4−14) Clusters: A Photoelectron Spectroscopy and Density-Functional Study. *J. Phys. Chem. A* **2003**, *107*, 6168−6175.
(64) Xing, X.; Yoon, B.; Landman, U.; Parks, J. H. Structural evolution of Au nanoclusters: From planar to cage to tubular motifs. *Phys. Rev. B* **2006**, *74*, 165423−165429.
(65) Perdew, J. P.; Schmidt, K. Jacob's ladder of density functional approximations for the exchange-correlation energy. Density Functional Theory and Its Application to Materials. *AIP Conf. Proc.* **2001**, *577*, 1−20.
(66) Peverati, R.; Truhlar, D. G. Exchange-Correlation Functional with Good Accuracy for Both Structural and Energetic Properties while Depending Only on the Density and Its Gradient. *J. Chem. Theory Comput.* **2012**, *8*, 2310−2319.
(67) Sun, J.; Marsman, M.; Csonka, G. I.; Ruzsinszky, A.; Hao, P.; Kim, Y.-S.; Kresse, G.; Perdew, J. P. Self-consistent meta-generalized gradient approximation within the project-oraugmented-wave method. *Phys. Rev. B* **2011**, *84*, 035117−035129.
(68) Mantina, M.; Valero, R.; Truhlar, D. G. Validation study of the ability of density functionals to predict the planar-to-three-dimensional structural transition in anionic gold clusters. *J. Chem. Phys.* **2009**, *131*, 064706−064711.
(69) Ferrighi, L.; Hammer, B.; Madsen, G. K. H. 2D-3D Transition for Cationic and Anionic Gold Clusters: A Kinetic Energy Density Functional Study. *J. Am. Chem. Soc.* **2009**, *131*, 10605−10609.